CMI

www.nature.com/cmi

ARTICLE

Kupffer cell restoration after partial hepatectomy is mainly driven by local cell proliferation in IL-6-dependent autocrine and paracrine manners

Yeni Ait Ahmed[1,2], Yaojie Fu[1], Robim M. Rodrigues[1], Yong He[1], Yukun Guan[1], Adrien Guillot[1], Ruixue Ren[1], Dechun Feng[1], Juan Hidalgo[3], Cynthia Ju[4], Fouad Lafdil[2,5,6]✉ and Bin Gao[1]✉

Kupffer cells (KCs), which are liver-resident macrophages, originate from the fetal yolk sac and represent one of the largest macrophage populations in the body. However, the current data on the origin of the cells that restore macrophages during liver injury and regeneration remain controversial. Here, we address the question of whether liver macrophage restoration results from circulating monocyte infiltration or local KC proliferation in regenerating livers after partial hepatectomy (PHx) and uncover the underlying mechanisms. By using several strains of genetically modified mice and performing immunohistochemical analyses, we demonstrated that local KC proliferation mainly contributed to the restoration of liver macrophages after PHx. Peak KC proliferation was impaired in *Il6*-knockout (KO) mice and restored after the administration of IL-6 protein, whereas KC proliferation was not affected in *Il4*-KO or *Csf2*-KO mice. The source of IL-6 was identified using hepatocyte- and myeloid-specific *Il6*-KO mice and the results revealed that both hepatocytes and myeloid cells contribute to IL-6 production after PHx. Moreover, peak KC proliferation was also impaired in myeloid-specific *Il6* receptor-KO mice after PHx, suggesting that IL-6 signaling directly promotes KC proliferation. Studies using several inhibitors to block the IL-6 signaling pathway revealed that sirtuin 1 (SIRT1) contributed to IL-6-mediated KC proliferation in vitro. Genetic deletion of the *Sirt1* gene in myeloid cells, including KCs, impaired KC proliferation after PHx. In conclusion, our data suggest that KC repopulation after PHx is mainly driven by local KC proliferation, which is dependent on IL-6 and SIRT1 activation in KCs.

Keywords: IL-6; Sirtuin 1; Liver regeneration; Kupffer cells; Myeloid cells

Cellular & Molecular Immunology (2021) 18:2165–2176; https://doi.org/10.1038/s41423-021-00731-7

INTRODUCTION

The liver has the unique capability to regenerate after injury or partial resection. These regenerative functions are orchestrated by a variety of immune cells and mediators produced by these cells [1, 2]. The liver is considered an immunological organ because it contains a high density of immune cells, such as resident macrophages known as Kupffer cells (KCs), innate immune cells (e.g., NK and NKT cells), and lymphoid immune cells, including T and B lymphocytes [3, 4]. Among these cells, KCs represent one of the largest macrophage populations in the human body [5] and represent ~30% of hepatic nonparenchymal cells [6]. Because KCs play a wide variety of roles in metabolism, toxin clearance, immunity, and inflammation, their quick restoration is critical in the clinical care of liver diseases, including injury mediated by alcohol, lipids, drugs, toxins, viruses, bacteria, and ischemia, to ensure hepatic regeneration [7–10]. However, the origin of these cells and the underlying mechanisms leading to their restoration remain largely unclear or controversial.

Alongside resident KCs, which are derived from the fetal yolk sac, bone marrow-derived monocytes circulate through the hepatic vascular network in a steady state as patrolling cells and infiltrate the liver tissue upon injury [7, 8, 11]. Recently, several markers have been identified to discriminate between KCs and infiltrating macrophages. Ionized calcium-binding adapter molecule 1 (IBA1) has been described as a common marker of both monocytes and KCs, as well as monocyte and macrophage populations found in other organs in the body, such as microglia [12]. However, C-type lectin domain family 4 member F (CLEC4F) has been identified as the most specific KC marker to date, as it is not expressed by monocytes. KCs are commonly described as $CD45^{+}F4/80^{+}CD11b^{intermediate}CLEC4F^{+}$ cells [13, 14]. In contrast, CX3CR1, the G-protein-coupled fractalkine receptor, is expressed by monocytes and capsular macrophages and is absent from KCs

[1]Laboratory of Liver Diseases, National Institute on Alcohol Abuse and Alcoholism, National Institutes of Health, Bethesda, MD, USA. [2]Université Paris-Est-Créteil, Créteil, France. [3]Universitat Autònoma de Barcelona, Barcelona, Spain. [4]Department of Anesthesiology, McGovern Medical School, University of Texas Health Science Center at Houston, Houston, TX, USA. [5]INSERM U955, Institut Mondor de Recherche Biomédicale, Créteil, France. [6]Institut Universitaire de France (IUF), Paris, France. ✉email: fouad.lafdil@inserm.fr; bgao@mail.nih.gov

Received: 12 January 2021 Accepted: 22 June 2021
Published online: 19 July 2021

[15]. The identification of these markers has led to improved characterization of hepatic macrophage populations, and emerging evidence suggests that while at a steady-state, most macrophages in the liver are KCs, and following tissue damage and inflammation, which causes a loss of KCs, circulating monocytes infiltrate the hepatic parenchyma. For example, a decrease in liver KCs has been reported in several types of fulminant hepatitis, including infection with murine cytomegalovirus [16] or the bacterium *Listeria monocytogenes* [17], and in models of methionine/choline-deficient (MCD) diet-induced nonalcoholic steatohepatitis (NASH) [18] and hepatocellular carcinoma (HCC) [19]. Several studies have suggested that these lost KCs are partially replaced by circulating monocytes [17, 20–23]. However, whether local KC proliferation or circulating monocytes restore liver macrophages after partial hepatectomy (PHx) remains unclear.

The liver has a remarkable ability to regenerate after tissue loss (such as PHx) or injury [24, 25]. Previous studies suggested that PHx triggers the activation of KCs, and these cells start producing cytokines such as tumor necrosis factor α (TNF-α) and interleukin 6 (IL-6) that stimulate hepatocyte proliferation [24, 25] and finely regulate liver regeneration to reach a stable liver mass [26]. Although the mechanisms of hepatocyte proliferation have been well described [27], the underlying mechanisms involved in macrophage replenishment remain unclear. As macrophages orchestrate liver regeneration and interact with other hepatic cells in regenerating livers through the production of cytokines [28–30], it is crucial to restoring their pool to sustain the regenerative process. In fact, studies have shown that liver regeneration is severely impaired when macrophages are depleted [31, 32]. Among several cytokines produced by the liver during regenerative processes, IL-6 is known to be a key regulator of hepatic parenchyma restoration [29, 33]. Indeed, deletion of the *Il6* gene has been shown to cause liver failure in mice after PHx [34]. Interestingly, IL-6 is a cytokine that targets several types of hepatic cells in addition to hepatocytes during regeneration [35, 36]. The IL-6 receptor is composed of two subunits, IL-6Rα and gp130. While gp130 is ubiquitously expressed in the body, IL-6Rα is only expressed by a few cell types, including hepatocytes, KCs, hepatic stellate cells, and biliary cells [35, 36]. In addition, IL-6 can also bind to soluble IL-6Rα to form a more stable IL-6/IL-6Rα complex, which can in turn bind to gp130 expressed on the cell membrane. This alternative pathway is called IL-6 trans-signaling and is particularly important for IL-6 signaling in cells that do not express transmembrane IL-6Rα. This trans-signaling pathway has been associated with better liver regenerative capacities [37, 38]. However, little information is available about the potential impact of IL-6 on KCs during liver regeneration following PHx.

In the current study, no apoptosis was observed in KCs in the remnant liver after PHx, and the restoration of KCs during liver regeneration in this model mainly originated from the local proliferation of the remaining KCs, which occurred in an IL-6-dependent manner through the activation of SIRT1. Finally, both hepatocytes and myeloid cells contribute to IL-6 production after PHx.

MATERIALS AND METHODS

Animals

Il6-KO, *Il4*-KO, *Csf2*-KO, and *Ccr2*-KO mice on a C57BL/6J background and wild-type C57BL/6J mice were purchased from the Jackson Laboratory (Maine, ME). $Lyz^{Cre/Cre}$, $Alb^{Cre/Cre}$, and $Cx3cr1^{GFP}$ knock-in/knock-out mice were also purchased from Jackson Laboratory. Homozygous $Cx3cr1^{GFP/GFP}$ mice were bred with C57BL/6J mice to obtain heterozygous $Cx3cr1^{GFP/-}$ mice. Mice with myeloid-specific deletion of the *Il6r* gene ($Il6r^{Mye}$-KO) were generated through several steps of crossing $Il6r^{f/f}$ mice with $Lyz^{Cre/Cre}$ mice as described previously [39]. $Il6^{f/f}$ mice were generated as previously described [40]. Mice with myeloid-specific deletion of the *Il6* gene ($Il6^{Mye}$-KO) and hepatocytes ($Il6^{Hep}$-KO) were generated through several steps of crossing $Il6^{f/f}$ mice with $Lyz^{Cre/Cre}$ and $Alb^{Cre/Cre}$ mice, respectively. The AlbCre line has been widely used to delete genes of interest in hepatocytes, and we have previously demonstrated that hepatocyte *Il6* was effectively deleted in $Il6^{Hep}$-KO mice [41]. Effective deletion of *Il-6* in KCs from $Il6^{Mye}$-KO mice was confirmed in the current study (see Results section). Myeloid-specific *Sirt1*-knockout ($Sirt1^{Mye}$-KO) mice were kindly provided by Dr. Xiaoling Li (NIEHS, NIH) as described previously [42].

Eight- to twelve-week-old mice were used for PHx. Free access to food and water was offered to the animals, and bacon softies were added on the floor for all animals after surgery. PHx was performed between 8 a.m. and 1 p.m. under sterile conditions. The animals were anesthetized with isoflurane, and buprenorphine (0.6 μg/g) was injected subcutaneously on the left side of the abdomen. Alcohol and betadine were applied to the abdominal skin of the animals prior to midline laparotomy. The left and middle lobes of the liver, along with the gall bladder, were consecutively ligated at the base and resected. The abdominal wall and the skin were sutured separately. BrdU (Sigma-Aldrich, St. Louis, MO) was injected intraperitoneally (50 μg/g) 2 h before sacrifice. When indicated, recombinant IL-6 (2 μg/g) was injected intraperitoneally. Recombinant human IL-6 was produced through recombinant DNA technology and purified as described previously [43].

All animals received humane care in accordance with the Guide for the Care and Use of Laboratory Animals published by the National Institutes of Health, and all animal experiments were approved by the NIAAA Animal Care and Use Committee.

KC isolation

KCs were isolated from mouse livers as described by Marcela Aparicio-Vergara et al. [44]. The liver was first perfused with 50 mL of EGTA, followed by 50 mL of collagenase type I (0.075% in 1× HBSS) perfusion solution. After perfusion, the liver was triturated and further digested with a collagenase type I digestion solution (0.015%) for 10–20 min at 37 °C on a shaker (90 rpm). The obtained suspension was then filtered through a 70 μm nylon mesh and centrifuged for 5 min at 50 g. The supernatant containing the nonparenchymal cells was centrifuged at 500 g for 10 min. The cell pellet was then resuspended in 8 mL of 40% Percoll, topped with 4 mL of HBSS, and then centrifuged at 1150 g for 17 min at 4 °C. The interphase containing the nonparenchymal cells was collected, washed with 1× HBSS, and pelleted by centrifugation for 10 min at 500 g. The obtained cell pellet was further processed by magnetic cell sorting (MACS) (endothelial cell marker CD146 MicroBeads, Miltenyi) to remove sinusoidal endothelial cells as described by the supplier's instructions. The CD146-negative cell fraction was seeded in 6-well plates and cultured for 1 h in RPMI supplemented with FBS (10%), penicillin (100 U/mL), and streptomycin (100 μg/mL). Nonadherent cells were removed by washing, and the adherent cells represented purified KC (KC purity reached ~80%).

Cell culture

Freshly isolated KCs and the RAW264.7 mouse macrophage cell line (ATCC, Manassas, VA) were cultured in RPMI + 10% FBS and were serum-deprived for proliferation assays. The inhibitors used in this study were 200 μM EX-527 (SIRT-1), 20 μM SB203580 (P38/AKT), 100 μM PD98059 (MAPK/ERK), and 100 μM SP600125 (JNK) (Selleck Chemicals Llc, Houston, TX). When indicated, cells were stimulated by the addition of rIL-6 (100 ng/ml) to the medium.

SIRT1 activity assay

RAW cell nuclei were extracted using the NE-PER nuclear and cytoplasmic extraction kit (Thermo Scientific, Waltham, MA) and were further processed to collect nuclear SIRT1 and assess enzymatic activity using the SIRT1 activity assay kit (Abcam, Cambridge, UK) according to the manufacturer's protocol.

Immunofluorescent staining

Livers were collected after the mice were euthanized and were placed in formalin for fixation. The tissues were dehydrated in ethanol solutions and then embedded in paraffin. Tissues were sectioned one day prior to staining and dried at 37 °C. Deparaffinization and rehydration of the microsections were performed using xylene and ethanol solutions with decreasing concentrations. Tissue sections were exposed to primary antibodies overnight at 4 °C, and secondary antibodies were applied for 1 h at room temperature the following day after three washes with PBS. The following antibodies were used: IBA1 (Abcam, Cambridge, UK), CLEC4F

(Cell Signaling, Danvers, MA), F4/80 (Cell Signaling, Danvers, MA), anti-rabbit Alexa Fluor 488 (#4412), anti-rat Alexa Fluor 555 (#4417) (Cell Signaling), and streptavidin-conjugated 555 (#S21381) (ThermoFisher, Waltham, MA).

BrdU staining was performed using the BrdU In Situ Detection Kit (#551321) (BD Pharmingen, San Jose, CA). Biotinylated anti-BrdU primary antibodies were applied overnight at 4 °C after a blocking step with goat serum for 1 h. The following day, the liver tissue sections were washed and incubated with streptavidin-coupled secondary antibodies for 1 h.

ELISA

Blood was collected retroorbitally from the mice at the indicated times post-PHx. Serum was separated by centrifugation. A mouse IL-6 ELISA kit (M6000B) from R&D Systems (Minneapolis, MN) was used to quantify serum IL-6 levels according to the manufacturer's instructions.

Mouse genotyping

For genotyping purposes, pieces of the ear were collected and digested using the DirectPCR Lysis Reagent (Ear) kit (Viagen Biotech, Los Angeles, CA). The genotyping protocol information is described on the Jax website. For *Il6*^{flox} mice, DNA was amplified using the following primers: *Il6*^{flox} forward CCCACCAAGAACGATAGTCA and reverse GGT ATC CTC TGT GAA GTC CTC.

RNA extraction and quantitative reverse transcription PCR (RT-qPCR)

For gene expression and RNA extraction, snap-frozen liver samples or freshly isolated KCs and RAW cells were placed in TRIzol reagent. Liver tissues were homogenized with beads in a TissueLyser and collected in TRIzol reagent. RNA was further extracted according to the Qiagen RNEasy Mini kit protocol and transcribed into cDNA. The primers used in this study were as follows: *Il6*: forward 5′–TCCATCCAGTTGCCTTCTTG–3′ and reverse 3′–TTCCACGATTTCCCAGAGAAC–5′; *Il4:* forward 5′–GGTCTCAACCCCCAGCT AGT–3′ and reverse 3′–GCCGATGATCTCTCTCAAGTGAT–5′; and *Csf2*: forward 5′–GGCCTTGGAAGCATGTAGAGG–3′ and reverse 3′–GGAGAACTCGTTAGAG ACGACTT–5′.

Statistical analysis

The results are expressed as the mean ± SEM, and statistical significance was determined by a two-tailed Student's *t*-test or one- or two-way analysis of variance as appropriate using PRISM 9.0 software. Significance between multiple groups was determined by ANOVA. Values of $P < 0.05$ were considered significant.

RESULTS

Liver KC restoration after PHx is mainly driven by local KC proliferation independent of circulating monocytes

To determine the kinetics of hepatocyte and macrophage proliferation, liver tissues were collected from 0 to 72 h after PHx, and bromodeoxyuridine (BrdU) incorporation was examined by immunofluorescence analysis (Fig. 1A). Hepatocyte proliferation peaked at 40 h after PHx (Fig. 1A, B), and ~30% of hepatocytes were BrdU$^+$. Next, proliferating macrophages were identified by double immunofluorescence staining for both IBA1 (a pan-macrophage marker) and BrdU (a proliferation marker), and the results revealed that liver macrophage proliferation peaked at 48 h after PHx (Fig. 1A, C). At the peak, ~22% of total macrophages were proliferating (Fig. 1C).

To address the question of whether the restoration of liver macrophages following PHx resulted from the recruitment of circulating monocytes or from resident KC proliferation, we performed double immunostaining with IBA1 and CLEC4F antibodies. IBA1 is expressed by both KCs and infiltrating monocytes, while CLEC4F is specifically expressed by KCs [13, 14]. At 48 h after surgery, immunohistochemical analysis of livers from sham or PHx mice revealed that more than 97% of all IBA1$^+$ macrophages in the liver also expressed CLEC4F (Fig. 1D, E), suggesting that macrophages in the liver at the peak of proliferation after PHx expressed the KC-specific marker CLEC4F, and very few CLEC4F$^-$ IBA1$^+$ infiltrating macrophages were observed.

To further support this conclusion, we used a murine model in which the green fluorescent protein (GFP) gene was inserted under the control of the *Cx3cr1* gene promotor to track the flow of circulating monocytes. GFP immunohistochemical staining (Fig. 1F) of liver tissue sections revealed that the number of GFP$^+$ infiltrating macrophages after PHx was low and similar to that in sham mice (Fig. 1G), suggesting that no significant monocyte infiltration occurred after PHx. Furthermore, we investigated whether impairments in circulating monocyte infiltration affected macrophage restoration after PHx. To address this question, *Ccr2*-KO mice in which the *Ccr2* gene, which encodes the key monocyte recruitment chemokine receptor CCR2, was deleted, were subjected to PHx. Immunofluorescence analysis of liver tissue sections revealed that both WT and *Ccr2*-KO mice had ~30% IBA1$^+$ BrdU$^+$ liver macrophages at 40 h and 48 h after PHx, and there were no differences between the two groups (Fig. 1H, I), suggesting that peak liver macrophage proliferation was not impacted when monocyte chemotaxis was disrupted.

Neither IL-4 nor colony-stimulating factor 2 (CSF2) is required for peak KC proliferation following PHx

Both IL-4 and CSF-2 (also known as a granulocyte-macrophage colony-stimulating factor; GM-CSF) has been suggested to play important roles in macrophage proliferation and KC renewal [45, 46]; therefore, we first tested whether IL-4 contributed to KC proliferation after PHx. As shown in Fig. 2A, hepatic expression of *Il4*, as detected by RT-qPCR, was comparable in sham and PHx mice. *Il4*-KO mice displayed a trend of lower KC proliferation at 40 h and 48 h after PHx than WT mice, but the difference was not statistically significant (Fig. 2B, C). Similarly, hepatic expression of *Csf2*, as detected by RT-qPCR, was also comparable in sham and PHx mice (Fig. 2D). Deletion of the *Csf2* gene in *Csf2*-KO mice did not affect KC proliferation post-PHx (Fig. 2E, F).

IL-6 is required for the peak KC proliferation following PHx

IL-6 has been shown to contribute to hepatocyte proliferation after PHx [47], and we then evaluated the potential impact of IL-6 on KC proliferation. Hepatic *Il6* mRNA expression levels were upregulated in both the sham and PHx groups, with much higher levels in the latter group (Fig. 3A). To investigate the role of IL-6 in hepatocyte and KC repopulation after PHx, WT, and *Il6*-KO mice were subjected to PHx, and hepatocyte and KC proliferation were assessed by immunofluorescence staining (Fig. 3B). All WT mice survived 48 h after PHx, while the survival rate in the *Il6*-KO group was 77%. The results showed that at 48 h, ~30% of hepatocytes were BrdU$^+$ in WT mice while proliferating hepatocytes did not exceed 10% in *Il6*-KO mice (Fig. 3B, C). Moreover, intravenous injection of recombinant IL-6 (rIL-6) in PHx *Il6*-KO mice partially restored hepatocyte proliferation (Fig. 3C), suggesting that IL-6 plays an important role in promoting hepatocyte proliferation. Next, we examined KC proliferation and found that 20% of IBA1$^+$ cells were BrdU$^+$ in WT mice, but these cells only accounted for 6% in *Il6*-KO mice (Fig. 3D). Intravenous injection of rIL-6 fully restored peak macrophage proliferation in PHx *Il6*-KO mice (Fig. 3D).

Both hepatocytes and KCs are major sources of IL-6 after PHx

To determine whether IL-6 was mainly produced by hepatocytes or myeloid cells, *Il6*^{Hep}-KO and *Il6*^{Mye}-KO cells were subjected to PHx. Effective deletion of *Il-6* in hepatocytes in *Il6*^{Hep}-KO mice was reported previously [41]. In addition, LyzCre has been used to effectively delete genes of interest in KCs by many labs, including ours [48]. Here, we further confirmed the efficacy of *Il6* deletion in KCs, which was assessed by isolating KCs from *Il6*$^{f/f}$ and *Il6*^{Mye}-KO mice injected with LPS, along with control *Il6*$^{f/f}$ mice injected with phosphate-buffered saline (PBS). As LPS is a powerful inducer of *Il6*

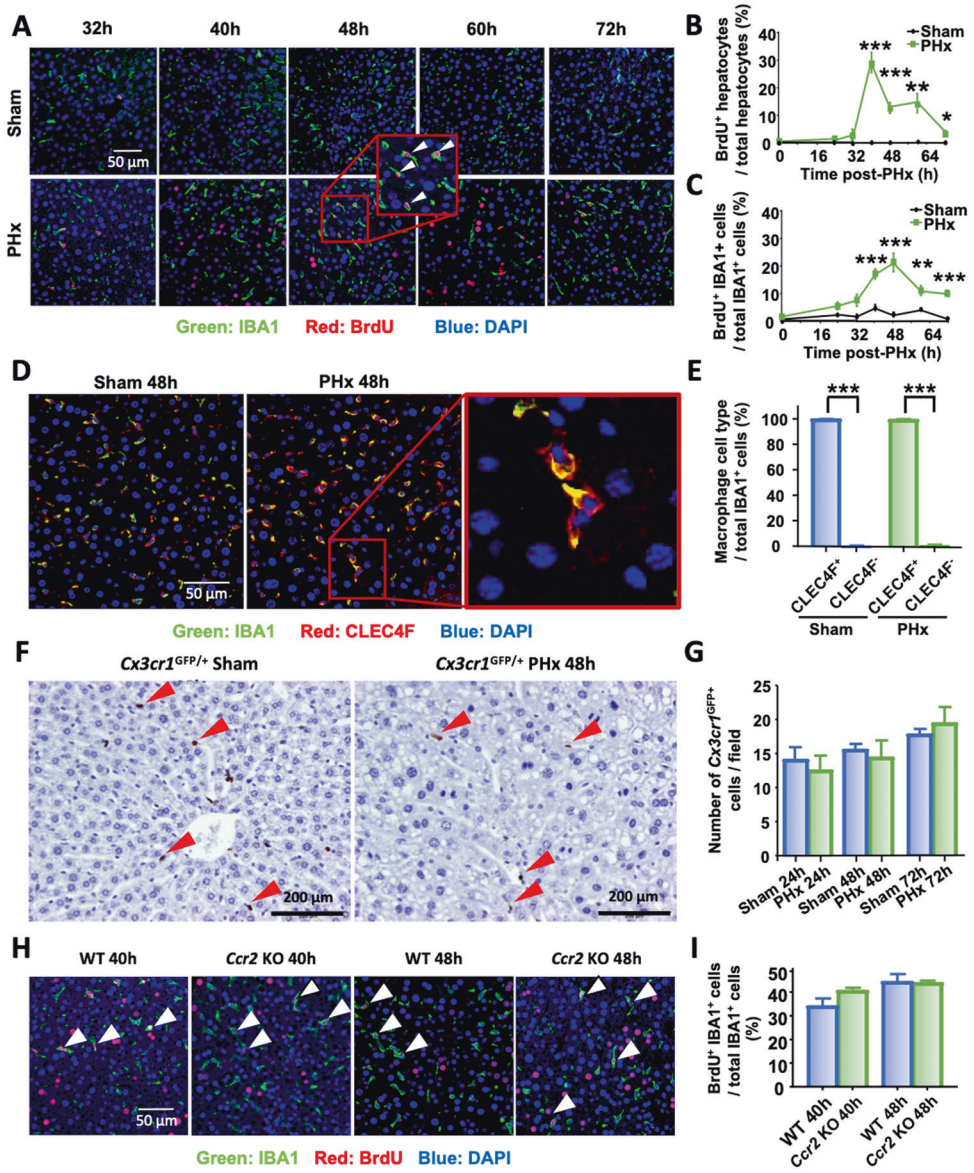

Fig. 1 Liver macrophage restoration after PHx is mainly driven by local KC proliferation. **A**–**C** Immunofluorescence analysis of liver tissue sections from sham and PHx mice ($n = 5$–6/group) 32 h to 72 h after surgery and stained with antibodies against IBA1 (green) and BrdU (red). Hepatocytes were identified by their large round nuclei, and macrophages were identified by IBA1 staining. Proliferating macrophages are highlighted by arrowheads. The quantification of hepatocyte and macrophage proliferation at the indicated time points is shown in panels (**B**) and (**C**). **D**, **E** IBA1 (green) and CLEC4F (red) immunofluorescence staining of liver tissue sections from sham and PHx mice 48 h after surgery ($n = 6$/group). Quantification of CLEC4F$^+$ and CLEC4F$^-$ cells among IBA1$^+$ cells in sham and PHx mice at 48 h is shown in panel (**E**). **F**, **G** GFP immunohistochemical staining of liver tissue sections from *Cx3cr1*$^{GFP/-}$ mice collected 48 h after surgery ($n = 6$/group). The number of CX3CR1^{GFP+} cells was counted and is shown in panel (**G**). Arrowheads represent CX3CR1^{GFP+} infiltrating monocytes. **H**, **I** Immunofluorescence analysis of liver tissue sections from WT and *Ccr2*-KO mice collected 40 h and 48 h after PHx ($n = 5$–6/group) and stained with antibodies against IBA1 (green) and BrdU (red). Arrowheads represent proliferating macrophages. Quantification of BrdU$^+$ IBA1$^+$ proliferating macrophages is shown in panel (**I**). BrdU was injected 2 h before sacrifice and is shown in panels (**A**) and (**H**). The values are expressed as the mean ± SEM. $^*P < 0.05$, $^{**}P < 0.01$, $^{***}P < 0.001$ in comparison to the corresponding sham groups in panels (**B**) and (**C**) and to CLEC4F$^-$ cells in panel (**E**)

expression, we showed that *Il6* mRNA levels were highly induced in KCs isolated from *Il6*$^{f/f}$ mice at 3 h after LPS injection compared to those of the PBS control group, while there was no induction of *Il6* mRNA levels in the *Il6*^{Mye}-KO mice injected with LPS (Fig. 4A). Sera were collected 3 h and 6 h following surgery and subjected to ELISA analysis of IL-6 levels. As shown in Fig. 4B, serum IL-6 concentrations were ~600 pg/mL in *Il6*$^{f/f}$ control mice, and these levels were significantly reduced to ~200 pg/mL in both *Il6*^{Hep}-KO and *Il6*^{Mye}-KO mice. In addition, more than 20% of KCs were proliferating (BrdU$^+$) in *Il6*$^{f/f}$ control mice at 48 h after PHx, while only ~15% of KCs were proliferating in *Il6*^{Hep}-KO or *Il6*^{Mye}-KO mice (Fig. 4C, D). Collectively, these data showed that both hepatocytes and KCs represent major sources of IL-6 that contribute to KC proliferation.

Disruption of IL-6 signaling in KCs impairs proliferation without triggering apoptosis after PHx

To determine whether IL-6 leads to KC proliferation by direct or indirect effects, mice with myeloid-specific *Il6r* deletion (*Il6r*^{Mye}-KO) were subjected to PHx. In the WT group, 100% of the mice

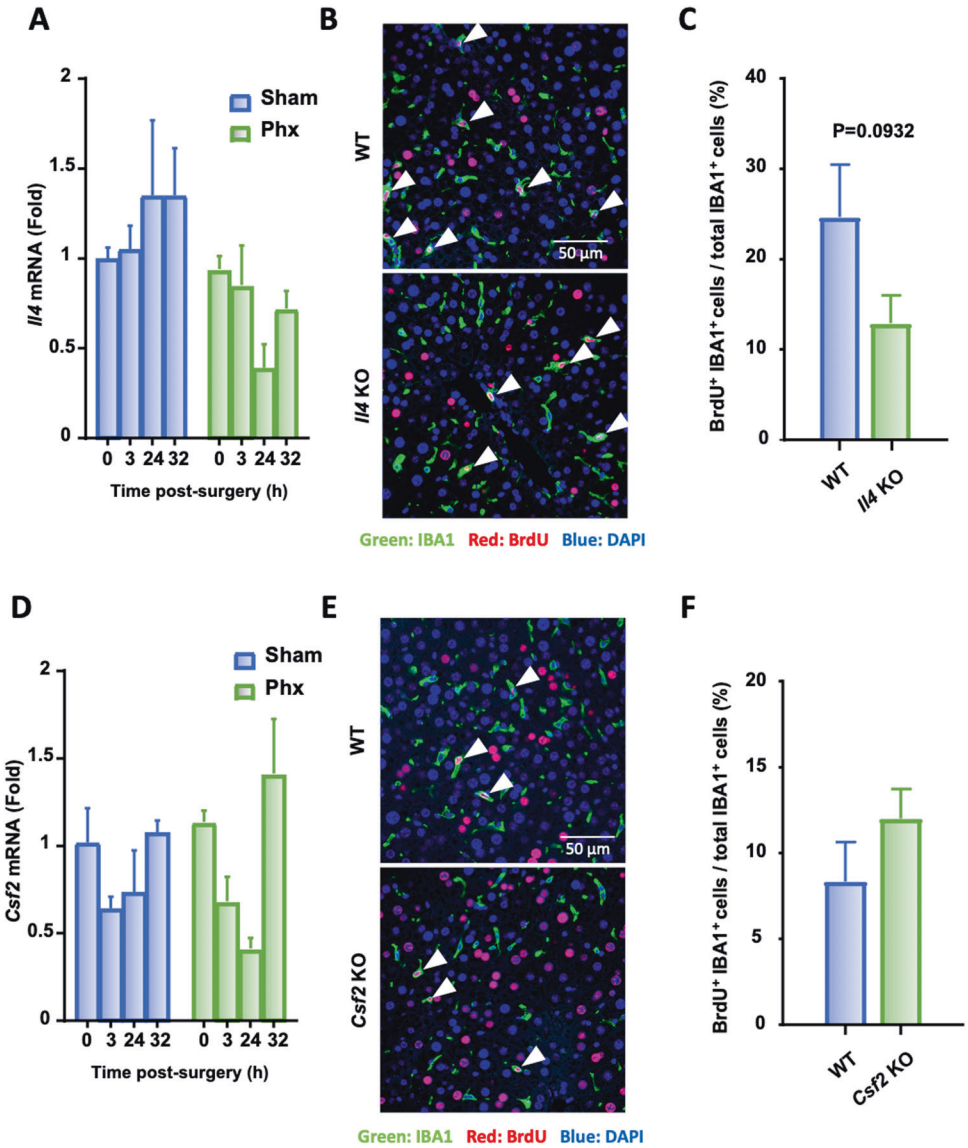

Fig. 2 IL-4 and CSF-2 are not required for the peak KC proliferation after PHx. **A** Kinetics of *Il4* mRNA expression in liver homogenates from WT and *Il4*-KO mice after PHx as determined by RT-qPCR. **B**, **C** Immunofluorescence analysis of liver tissue sections from WT and *Il4*-KO mice collected 48 h after PHx ($n = 6$/group) and stained with antibodies against IBA1 (green) and BrdU (red). Arrowheads represent proliferating KCs. The quantification of KC proliferation in WT and *Il4*-KO mice 48 h post PHx is shown in panel (**C**). **D** Kinetics of *Csf2* mRNA expression in liver homogenates from WT and *Csf2*-KO mice after PHx as determined by RT-qPCR. **E**, **F** Immunofluorescence analysis of liver tissue sections from WT and *Csf2*-KO mice collected 48 h after PHx ($n = 6$/group) and stained with antibodies against IBA1 (green) and BrdU (red). Arrowheads represent proliferating KCs. The quantification of KC proliferation in WT and *Csf2*-KO mice 48 h post PHx is shown in panel (**F**). The values are expressed as the mean ± SEM. BrdU was injected 2 h before sacrifice, as shown in panels (**B**) and (**E**)

survived 48 h post-PHx, while the survival rate was 85% in the $Il6r^{Mye}$-KO group ($n = 7$/group); however, no significant difference in the liver-to-body weight ratio was found between the two groups (Fig. 5A). Livers from PHx $Il6r^{f/f}$ and $Il6r^{Mye}$-KO mice were collected and subjected to immunofluorescence analysis to study hepatocyte and KC proliferation. As shown in Fig. 5B–D, hepatocyte proliferation, as determined by counting $BrdU^+$ hepatocytes, was comparable between $Il6r^{f/f}$ and $Il6r^{Mye}$-KO mice, while KC proliferation, as determined by counting IBA^+BrdU^+ cells, was significantly lower in $Il6r^{Mye}$-KO mice than in $Il6r^{f/f}$ control mice at 48 h after PHx. To determine whether this reduced number of accumulating KCs was due to increased apoptosis, we performed TUNEL staining on liver tissue sections and found few $TUNEL^+IBA1^+$ macrophages in either $Il6r^{f/f}$ or $Il6r^{Mye}$-KO mice at 48 h and 72 h post-PHx (Fig. 5E), suggesting that the reduced number of proliferating KCs in $Il6r^{Mye}$-KO mice was not due to enhanced macrophage apoptosis but rather to an impairment in proliferation.

IL-6 stimulates KC proliferation in vivo and in vitro

These data suggest that IL-6 signaling in KCs promotes KC proliferation after PHx. Next, we asked whether IL-6 directly stimulates KC proliferation in vivo in the absence of PHx. To answer this question, WT mice were treated with vehicle (PBS) or rIL-6. As shown in Fig. 6A, B, rIL-6 injection induced a significant increase in macrophage proliferation in the livers of WT mice in the absence of PHx, and no proliferating cells were detected after PBS injection. In addition, immunofluorescence analysis revealed that intravenous injection of rIL-6 preferentially induced $IBA1^+$ macrophage proliferation but not hepatocyte proliferation. To determine whether IL-6 signaling on KCs is required for IL-6-induced KC proliferation in vivo in the absence PHx, $Il6r^{f/f}$ mice

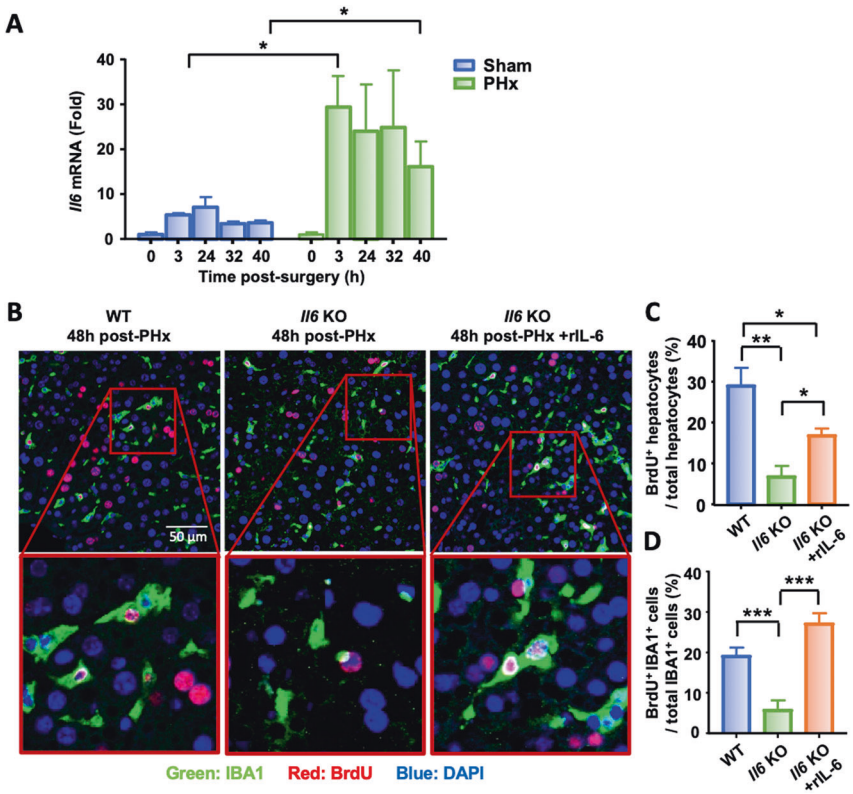

Fig. 3 IL-6 is required for proper KC proliferation after PHx. **A** Kinetics of *Il6* mRNA expression in liver homogenates from mice subjected to sham or PHx collected at the indicated time points and analyzed by RT-qPCR. **B**–**D** Immunofluorescence staining of liver tissue sections from WT, *Il6*-KO mice, and *Il6*-KO mice intravenously injected with rIL-6 and collected 48 h after PHx ($n = 6$–7/group). IBA1$^+$ (green) and BrdU$^+$ (red) cells indicate proliferating KCs. BrdU was injected 2 h before sacrifice, as shown in panel (**B**). The quantification of proliferating hepatocytes and KC 48 h post-PHx is shown in panels (**C**) and (**D**), respectively. The values are expressed as the mean ± SEM. *$P < 0.05$, **$P < 0.01$, ***$P < 0.001$

and *Il6r*^{Mye}-KO mice were treated with rIL-6 in the absence of PHx, and we found that macrophage proliferation reached 10% in *Il6r*$^{f/f}$ mouse livers, while this rate was 3% in *Il6r*^{Mye}-KO mice (Fig. 6C, D), suggesting that IL-6 directly stimulates KC proliferation in vivo by targeting IL-6R on KCs even under normal conditions without PHx.

To further decipher the direct impact of IL-6 on macrophage proliferation, RAW macrophages and freshly isolated KCs were stimulated with rIL-6 in vitro. Immunocytochemical analysis revealed a basal level of 22% of BrdU$^+$ RAW cells after 48 h of culture in the control condition (vehicle), which was significantly increased to 35% under rIL-6 stimulation (Fig. 6E, F). Similarly, in purified KC, rIL-6 was able to significantly increase their proliferation from 6% to 15% (Fig. 6G, H). These results reveal the direct proliferative effect of IL-6 on KCs in vivo and in vitro.

SIRT1 is involved in IL-6-mediated KC proliferation

To further investigate the underlying factors involved in the IL-6 signaling pathway leading to KC proliferation, several inhibitors of downstream signaling pathways, including SIRT1, p38/Akt, MAPK/ERK, and JNK, were used (Fig. 7A). As expected, rIL-6 induced RAW cell proliferation compared to of vehicle-treated cells. RAW cells exposed to both rIL-6 and a SIRT1 inhibitor showed significantly reduced proliferation compared to RAW cells exposed to rIL-6 alone after 6 h of culture (Fig. 7A). No significant difference was reported in response to the other inhibitors at either the 3 h or 6 h time points. Next, we measured SIRT1 activity in RAW cells exposed to rIL-6 and found that RAW macrophages stimulated with rIL-6 exhibited significantly higher SIRT1 activity than the controls (Fig. 7B). These results strongly suggest that IL-6 mediates KC proliferation in a SIRT1-dependent manner. To further confirm these results, mice with myeloid cell-specific deletion of the *Sirt1* gene (*Sirt1*^{Mye}-KO) were subjected to PHx. The liver weights at the time of sacrifice were measured and revealed that the liver-to-body weight ratio of *Sirt1*$^{f/f}$ control mice was ~2.8, which was significantly reduced to 2.1 in *Sirt1*^{Mye}-KO mice 48 h post PHx (Fig. 7C). In addition, liver regeneration was further examined by immunofluorescence analysis, and the results revealed that at 48 h post-PHx, the hepatocyte proliferation rate reached 20% in *Sirt1*$^{f/f}$ mice, which was slightly but significantly reduced to 17% in *Sirt1*^{Mye}-KO mice (Fig. 7D, E). Interestingly, while over 20% of KCs were BrdU$^+$ in *Sirt1*$^{f/f}$ mice 48 h after surgery, this proliferation rate significantly dropped to less than 5% in *Sirt1*^{Mye}-KO mice (Fig. 7D, F). Taken together, these results suggest that SIRT1 is required for proper KC proliferation mediated by IL-6 after PHx.

DISCUSSION

In response to tissue damage, the liver has the unique ability to undergo a regenerative process that is finely orchestrated by KCs to maintain its mass and functions [1, 2]. As the total number of KCs is dramatically reduced following liver resection or partial liver transplantation, it is vital to restore the pool of these cells. In the present study, we provided new insights that shed light on the origin of hepatic macrophages during liver regeneration after PHx and the underlying mechanisms of their restoration.

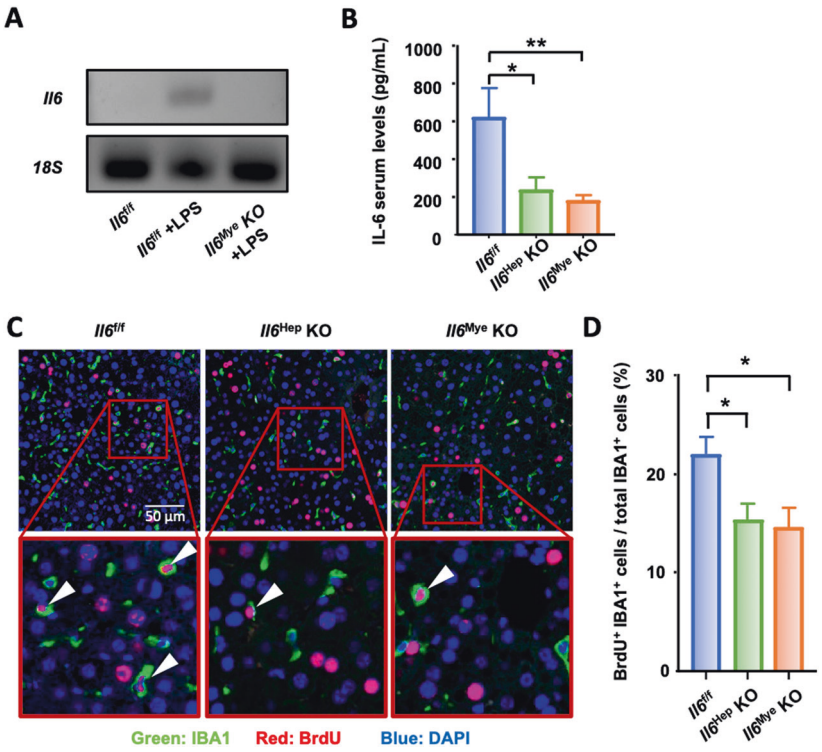

Fig. 4 Hepatocytes and KCs are important sources of IL-6 after PHx. **A** RT-qPCR confirming *Il6* deletion in KCs from *Il6*^{Mye}-KO mice. *Il6* mRNA expression in KCs isolated from control *Il6*$^{f/f}$ mice injected with PBS or LPS and *Il6*^{Mye}-KO mice injected with LPS (3 h injection). **B** Serum IL-6 levels in *Il6*$^{f/f}$, *Il6*^{Hep}-KO, and *Il6*^{Mye}-KO mice 3 h after PHx ($n = 6$/group). **C**, **D** Immunofluorescence analysis of liver tissue sections from *Il6*$^{f/f}$, *Il6*^{Hep}-KO, and *Il6*^{Mye}-KO mice collected 48 h after PHx ($n = 6$/group) and stained with anti-IBA1 (green) and BrdU (red) antibodies. BrdU was injected 2 h before sacrifice, as shown in panel (**C**). Arrowheads represent proliferating KCs. The quantification of macrophage proliferation in the liver 48 h after PHx is shown in panel (**D**). The values are expressed as the mean ± SEM. *$P < 0.05$, **$P < 0.01$

Liver KC restoration after PHx is predominantly driven by local KC proliferation with a minor contribution from circulating macrophages

In this study, we showed that macrophage proliferation peaked at 48 h post-PHx, a few hours after that of hepatocytes at 40 h. Whether new macrophages are derived from circulating monocytes or resident KCs after PHx was not clear. In fact, the origin of repopulating hepatic macrophages has remained controversial, as recent studies have provided conflicting data about the capacity of monocytes and KCs to give rise to a fully regenerated pool of liver macrophages after liver injury [7, 8]. These conflicting data might result from the different models used to investigate the origin of hepatic macrophages. In a study in which KCs were completely depleted from a healthy liver without PHx, KC restoration was achieved through bone marrow-derived monocyte recruitment and differentiation in the liver [49]. In another study in which all immune cells, including KCs, were depleted by nonlethal 5 Gy irradiation in mice before PHx, the authors suggested that monocytes were recruited into partially hepatectomized livers and played a pivotal role in accelerating liver regeneration [21]. However, under conditions in which residual KCs are preserved in the remaining part of the liver after PHx, we provided several lines of evidence suggesting that circulating monocytes are minor contributors to restoring the initial pool of KCs. First, after PHx, few CX3CR1-labeled monocytes were recruited to the regenerating livers. Second, *Ccr2* deficiency in mice, which is a key chemokine receptor for monocyte recruitment, led to normal KC repopulation after PHx. Third, most macrophages found in the liver at 48 h post-PHx, which was the peak of liver macrophage proliferation, were IBA$^+$CLEC4F$^+$ KCs, and few IBA$^+$CLEC4F$^-$ infiltrating monocytes were detected in the regenerating liver after PHx. Finally, CLEC4F$^+$ KCs were capable of self-proliferation following PHx. In the current study, we mainly examined peak KC proliferation and did not trace KCs at later time points post-PHx, so we cannot rule out the contribution of infiltrating macrophages to liver macrophage restoration in this model; however, we believe that the infiltrating macrophage contribution at later time points post-PHx is minor because the partially hepatectomized liver is associated with little inflammation or monocyte infiltration at later time points.

IL-6 plays an important role in promoting KC proliferation after PHx in autocrine and paracrine manners

Although PHx is not characterized by a strong inflammatory response, several cytokines that are involved in macrophage proliferation, such as IL-6, are elevated post PHx [2, 50]. In the current study, we demonstrated that after PHx, KC proliferation was impaired in *Il6*-KO mice but not in *Il4*-KO or *Csf2*-KO mice. The administration of rIL-6 by injection partially increased hepatocyte proliferation and, interestingly, fully restored KC proliferation in *Il6*-KO mice after PHx. Collectively, our data suggest that IL-6 but not IL-4 or CSF-2 plays a critical role in promoting KC proliferation after PHx.

Although the elevation in IL-6 after PHx has been well documented, the source of this cytokine during liver regeneration remains obscure. Previous studies suggested that PHx induces an increase in gut-derived LPS in the blood [51], which likely contributes to the increase in IL-6 after PHx because LPS is known to stimulate macrophages to produce IL-6. In addition, one study suggested that LPS can also stimulate hepatocytes to produce IL-6 [52]. However, the exact sources of IL-6 after PHx remain unclear. In the current study, we demonstrated that serum levels of IL-6 were reduced by ~50% in myeloid- and hepatocyte-specific *Il6*-KO

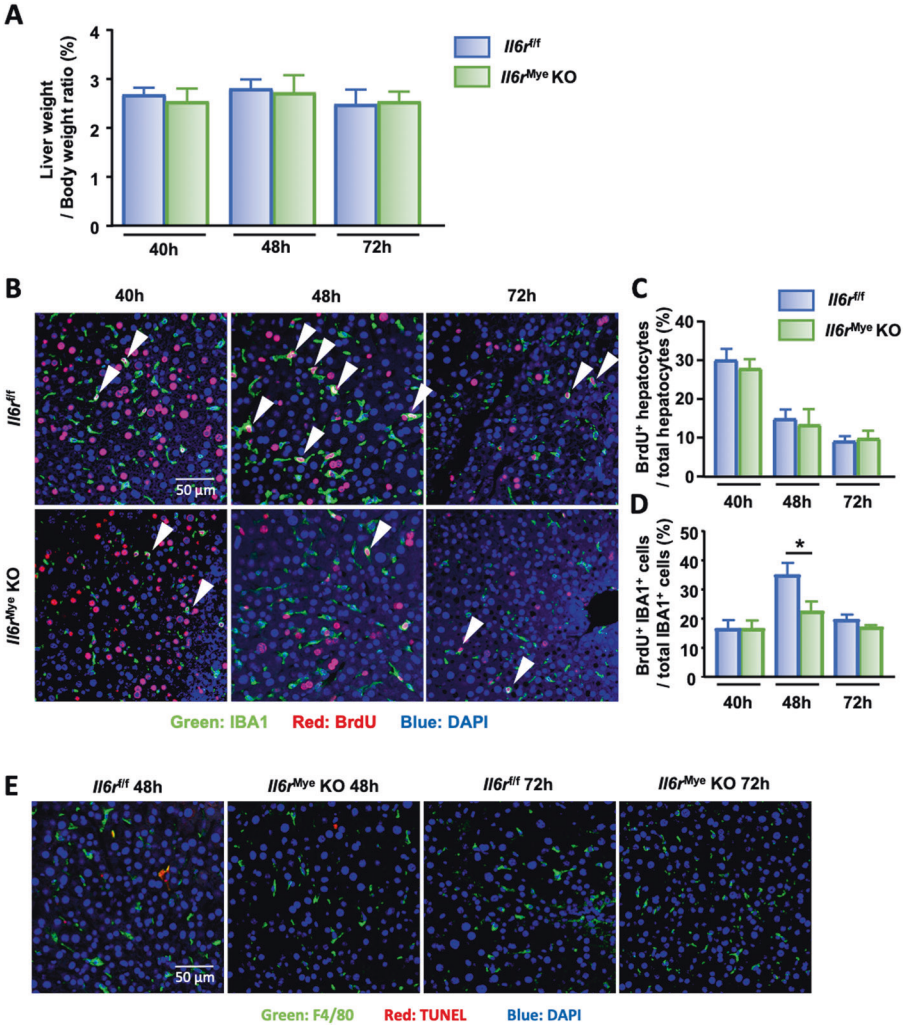

Fig. 5 Liver macrophage proliferation is impaired in Il6r^{Mye}-KO mice after PHx. **A** Liver-to-body weight ratios of *Il6r*$^{f/f}$ and *Il6r*^{Mye}-KO mice post-PHx. **B** Immunofluorescence analysis of liver tissue sections from *Il6r*$^{f/f}$ and *Il6r*^{Mye}-KO mice subjected to PHx ($n = 6$/group). Liver tissues were collected 40 h, 48 h, and 72 h after PHx and stained with antibodies targeting IBA1 (green) and BrdU (red). BrdU was injected 2 h before sacrifice. Arrowheads represent proliferating KCs. The quantification of hepatocyte and KC proliferation from panel **B** is shown in panels (**C**) and (**D**). **E** Immunofluorescence analysis of liver tissue sections from *Il6r*$^{f/f}$ and *Il6r*^{Mye}-KO mice 48 h and 72 h after PHx staining with anti-F4/80 and TUNEL antibodies. The values are expressed as the mean ± SEM. *$P < 0.05$

mice compared to WT mice after PHx. LyzCre and AlbCre mice have been well characterized and shown to efficiently and specifically delete the target genes in myeloid cells and hepatocytes in floxed mice, respectively. However, we cannot completely rule out the possibility that there are some partial leakages between these two Cre lines, although this possibility is low. Thus, the ~50% contribution of hepatocytes and myeloid cells to IL-6 production may be different from the true contribution from these cells. In conclusion, our data suggest that after PHx, not only do hepatocytes represent a source of IL-6 to promote KC proliferation in a paracrine manner, but KCs could also be considered an autocrine source of IL-6. Because KC and hepatocyte proliferation were significantly impaired in both *Il6*^{Mye}-KO and *Il6*^{Hep}-KO mice, it is plausible that KC and hepatocyte proliferation in double-mutant mice with *Il6* deletion in both hepatocytes and KCs will be further decreased compared to those in single-KO mice.

IL-6 promotes KC proliferation without affecting KC survival after PHx by enhancing SIRT1 activity

In the current study, we performed double immunofluorescence staining to clearly detect KC and macrophage proliferation in situ. By using this method, we demonstrated that KC proliferation was reduced in *Il6*-KO, hepatocyte- or myeloid-specific *Il6*-KO mice, and myeloid-specific *Il6r*-KO mice and that IL-6 stimulated KC and macrophage proliferation in vitro, clearly supporting a direct stimulatory effect of IL-6 on KC proliferation in vivo and in vitro. Flow cytometry experiments are an alternative method to detect KC proliferation and could also be performed to examine and confirm the role of IL-6 in KC proliferation in the future.

To explore the molecular mechanisms by which IL-6 stimulates KC proliferation, we used several inhibitors to block IL-6 downstream signaling pathways. Interestingly, among these inhibitors, the SIRT1 inhibitor showed the strongest inhibition of IL-6-induced KC proliferation in vitro. Furthermore, we demonstrated that genetic deletion of *Sirt1* in myeloid cells, including KCs, markedly reduced KC proliferation in vivo after PHx and impaired liver regeneration, as shown by the reduction in the liver-to-body weight ratio and hepatocyte proliferation in *Sirt1*^{Mye}-KO mice. In addition, IL-6 treatment directly increased SIRT1 activity in macrophages, suggesting that SIRT1 contributes to IL-6-induced KC proliferation during liver regeneration after PHx. A recent study also reported that SIRT1 plays a role in stimulating macrophage proliferation, as demonstrated by the findings that SIRT1

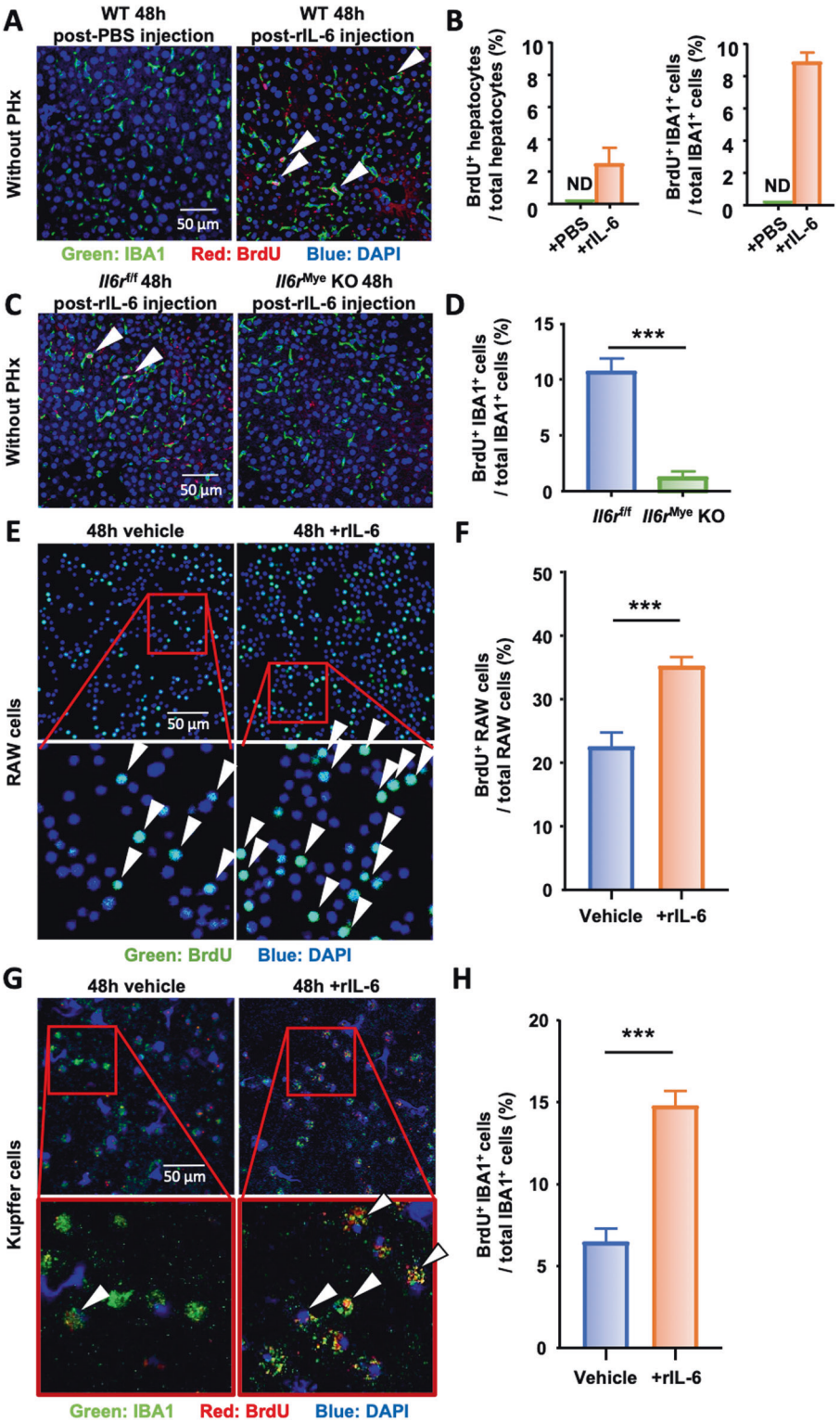

Fig. 6 IL-6 stimulates macrophage proliferation in vivo and in vitro. **A**, **B** Naïve wild-type mice (without PHx) were intravenously injected with PBS (control) or rIL-6, and liver tissues were collected 48 h after injection ($n = 7$/group) and subjected to immunofluorescence staining with antibodies against IBA1 (green) and BrdU (red). Arrowheads represent proliferating KC. The quantifications of $BrdU^+$ hepatocytes and $BrdU^+$ $IBA1^+$ cells are shown in panel B. ND: not detected. **C**, **D** $Il6r^{f/f}$ and $Il6r^{Mye}$-KO mice without PHx were intravenously injected with rIL-6 ($n = 7$/group), and liver tissues were collected 48 h after injection and subjected to immunofluorescence staining with antibodies against IBA1 (green) and BrdU (red). Arrowheads represent proliferating KC. The quantification of proliferating KCs in livers from $Il6r^{f/f}$ and $Il6r^{Mye}$-KO mice 48 h after intravenous injection of rIL-6 is shown in panel (**D**). **E**, **F** Immunofluorescence staining of RAW cells 48 h after exposure to rIL-6 or control medium (vehicle) with antibodies against BrdU (green). Proliferating RAW cells are identified by arrowheads. The quantification of proliferating RAW cells is shown in panel (**F**). **G**, **H** Immunofluorescence staining of freshly isolated KCs 48 h after exposure to rIL-6 or control medium (vehicle) with antibodies against IBA1 (green) and BrdU (red). The arrowheads represent proliferating KC. The quantification of KC proliferation is shown in panel (**H**). BrdU was injected 2 h before sacrifice in panels (**A**) and (**C**) and was added to the culture medium 2 h before collecting the cells in panels (**E**) and (**G**). The values are expressed as the mean ± SEM. ***$P < 0.001$

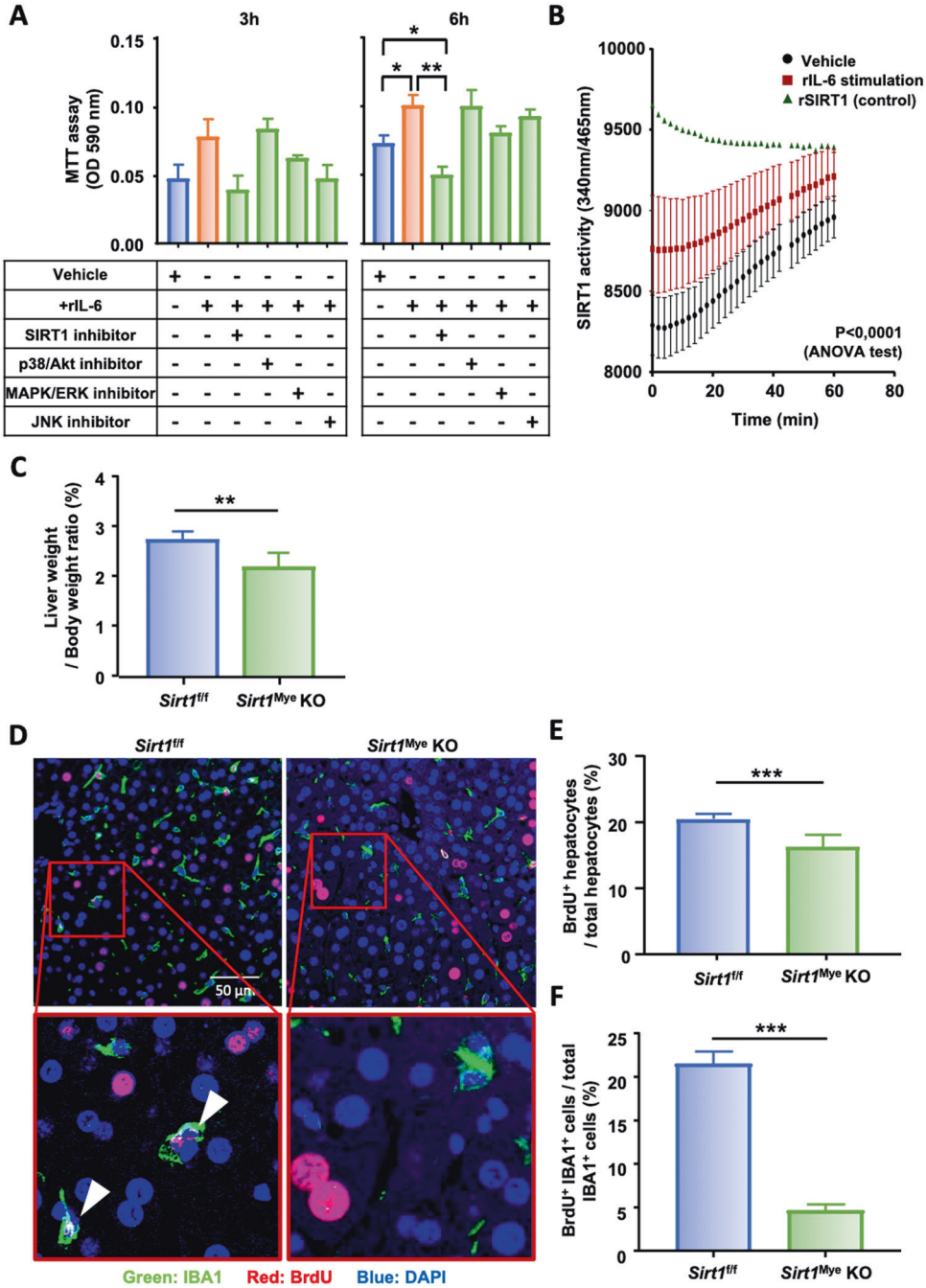

Fig. 7 IL-6 stimulates KC proliferation by inducing SIRT1 intracellular mechanisms following PHx. **A** RAW cell proliferation was analyzed by MTT assays 3 h and 6 h after exposure to recombinant IL-6 (rIL-6) and the indicated inhibitors or the vehicle control. **B** SIRT1 enzymatic activity in RAW cells after exposure to rIL-6 or control medium. Recombinant SIRT1 (rSIRT1) activity was included as a positive control. **C** Liver-to-body weight ratios of *Sirt1*$^{f/f}$ and *Sirt1*^{Mye}-KO mice that were sacrificed 48 h post-PHx. **D** Immunofluorescence staining of liver tissue sections from *Sirt1*$^{f/f}$ and *Sirt1*^{Mye}-KO mice 48 h after PHx ($n = 6$/group) with antibodies against IBA1^{+} (green) and BrdU^{+} (red). Arrowheads represent proliferating KCs. The quantification of proliferating hepatocytes and KCs from panel (**D**) is shown in panels (**E**) and (**F**). The values are expressed as the mean ± SEM. *$P < 0.05$, **$P < 0.01$, ***$P < 0.001$

overexpression via transfection of *Sirt1* into bone marrow-derived macrophages was associated with increased macrophage proliferation in vitro, whereas SIRT1 blockade by CRISPR/Cas9 gene editing or by nicotinamide injection in mice impaired alveolar and peritoneal macrophage self-renewal capacities [53]. Interestingly, previous studies on the PHx model have reported that age-related SIRT1 reductions and SIRT1 inhibition by short-interfering RNA (siRNA) were associated with less efficient liver regeneration (hepatocyte proliferation) after PHx [54]. Collectively, SIRT1 not only promotes KC renewal but also stimulates hepatocyte proliferation after PHx.

In addition to promoting macrophage proliferation, IL-6 signaling also plays an important role in enhancing macrophage survival [55]. However, in the current study, no enhanced KC apoptosis was observed in myeloid cell-specific *Il6r*-knockout mice compared to WT mice, suggesting that IL-6 is not required for KC survival after PHx or,

alternatively, that IL-6 trans-signaling might be contributing to this effect. Indeed, the IL-6 receptor (IL-6R) exists in two forms: a transmembrane receptor (mIL-6R) and a soluble receptor (sIL-6R). By binding to mIL-6R, IL-6 activates the canonical signaling pathway and predominantly triggers subsequent anti-inflammatory responses. On the other hand, in cells that do not express mIL-6R, IL-6 can activate the trans-signaling pathway by binding to sIL-6R [55]. Interestingly, our recent studies demonstrated that IL-6 signaling was required for infiltrating macrophage survival but not KC survival in the livers of high-fat diet-fed mice [39]. Taken together, these findings suggest that IL-6 is required for KC proliferation but not KC survival after PHx, which is probably because long-lived KCs do not need IL-6 signaling for survival.

In conclusion, our findings provide new insights into the origin of KCs in the regenerating liver after PHx, showing local proliferation of the remaining KCs independent of circulating monocytes. During this process, KC proliferation is partly controlled by IL-6 produced by both hepatocytes and KCs in regenerating livers, and IL-6 stimulates KC proliferation by increasing SIRT1 activity. Future studies on the interaction between IL-6 and other cytokines and growth factors, such as hepatocyte growth factor, which is known to be involved in hepatocyte proliferation after PHx, could provide additional insights into the mechanisms associated with KC proliferation.

REFERENCES

1. Dong Z, Wei H, Sun R, Tian Z. The roles of innate immune cells in liver injury and regeneration. Cell Mol Immunol. 2007;4:241–52.
2. Markose D, Kirkland P, Ramachandran P, Henderson NC. Immune cell regulation of liver regeneration and repair. J Immunol Regen Med. 2018;2:1–10.
3. Gao B, Jeong W-I, Tian Z. Liver: an organ with predominant innate immunity. Hepatology. 2008;47:729–36.
4. Heymann F, Tacke F. Immunology in the liver—from homeostasis to disease. Nat Rev Gastroenterol Hepatol. 2016;13:88–110.
5. Merlin S, Bhargava KK, Ranaldo G, Zanolini D, Palestro CJ, Santambrogio L, et al. Kupffer cell transplantation in mice for elucidating monocyte/macrophage biology and for potential in cell or gene therapy. Am J Pathol. 2016;186:539–51.
6. Nguyen-Lefebvre AT, Horuzsko A. Kupffer cell metabolism and function. J Enzymol Metab. 2015;1:101.
7. Wen Y, Lambrecht J, Ju C, Tacke F. Hepatic macrophages in liver homeostasis and diseases-diversity, plasticity and therapeutic opportunities. Cell Mol Immunol. 2021;18:45–56.
8. Krenkel O, Tacke F. Liver macrophages in tissue homeostasis and disease. Nat Rev Immunol. 2017;17:306–21.
9. Cai J, Zhang X-J, Li H. The role of innate immune cells in nonalcoholic steatohepatitis. Hepatology. 2019;70:1026–37.
10. Wang H, Mehal W, Nagy LE, Rotman Y. Immunological mechanisms and therapeutic targets of fatty liver diseases. Cell Mol Immunol. 2021;18:73–91.
11. Tacke F, Zimmermann HW. Macrophage heterogeneity in liver injury and fibrosis. J Hepatol. 2014;60:1090–6.
12. Guillot A, Buch C, Jourdan T. Kupffer cell and monocyte-derived macrophage identification by immunofluorescence on formalin-fixed, paraffin-embedded (FFPE) mouse liver sections. In: Aouadi M, Azzimato V (eds). Kupffer cells: methods and protocols. New York, NY: Springer US, 2020, pp 45–53.
13. Hsieh S-LE, Yang C-Y. CLEC4F, a Kupffer cells specific marker, is critical for presentation of alfa-galactoceromide to NKT cells. J Immunol. 2009;182:78.
14. Yang C-Y, Chen J-B, Tsai T-F, Tsai Y-C, Tsai C-Y, Liang P-H, et al. CLEC4F is an inducible C-type lectin in F4/80-positive cells and is involved in alpha-galactosylceramide presentation in liver. PLoS ONE. 2013;8:e65070–e65070.
15. Yona S, Kim K-W, Wolf Y, Mildner A, Varol D, Breker M, et al. Fate mapping reveals origins and dynamics of monocytes and tissue macrophages under homeostasis. Immunity. 2013;38:79–91.
16. Borst K, Frenz T, Spanier J, Tegtmeyer P-K, Chhatbar C, Skerra J, et al. Type I interferon receptor signaling delays Kupffer cell replenishment during acute fulminant viral hepatitis. J Hepatol. 2018;68:682–90.
17. Blériot C, Dupuis T, Jouvion G, Eberl G, Disson O, Lecuit M. Liver-resident macrophage necroptosis orchestrates type 1 microbicidal inflammation and type-2-mediated tissue repair during bacterial infection. Immunity. 2015;42:145–58.
18. Devisscher L, Scott CL, Lefere S, Raevens S, Bogaerts E, Paridaens A, et al. Non-alcoholic steatohepatitis induces transient changes within the liver macrophage pool. Cell Immunol. 2017;322:74–83.
19. Lefere S, Degroote H, Van Vlierberghe H, Devisscher L. Unveiling the depletion of Kupffer cells in experimental hepatocarcinogenesis through liver macrophage subtype-specific markers. J Hepatol. 2019;71:631–3.
20. Zigmond E, Samia-Grinberg S, Pasmanik-Chor M, Brazowski E, Shibolet O, Halpern Z, et al. Infiltrating monocyte-derived macrophages and resident Kupffer cells display different ontogeny and functions in acute liver injury. J Immunol. 2014;193:344–53.
21. Nishiyama K, Nakashima H, Ikarashi M, Kinoshita M, Nakashima M, Aosasa S, et al. Mouse CD11b+Kupffer cells recruited from bone marrow accelerate liver regeneration after partial hepatectomy. PLoS ONE. 2015;10:e0136774.
22. Reid DT, Reyes JL, McDonald BA, Vo T, Reimer RA, Eksteen B. Kupffer cells undergo fundamental changes during the development of experimental NASH and are critical in initiating liver damage and inflammation. PLoS ONE. 2016;11:e0159524.
23. Tran S, Baba I, Poupel L, Dussaud S, Moreau M, Gélineau A, et al. Impaired Kupffer cell self-renewal alters the liver response to lipid overload during non-alcoholic steatohepatitis. Immunity. 2020;53:627–40.
24. Elchaninov AV, Fatkhudinov TK, Usman NY, Kananykhina EY, Arutyunyan IV, Makarov AV, et al. Dynamics of macrophage populations of the liver after subtotal hepatectomy in rats. BMC Immunol. 2018;19:23.
25. Fausto N, Campbell JS, Riehle KJ. Liver regeneration. Hepatology. 2006;43:S45–S53.
26. Ichikawa T, Zhang Y-Q, Kogure K, Hasegawa Y, Takagi H, Mori M, et al. Transforming growth factor β and activin tonically inhibit DNA synthesis in the rat liver. Hepatology. 2001;34:918–25.
27. Weglarz TC, Sandgren EP. Timing of hepatocyte entry into DNA synthesis after partial hepatectomy is cell autonomous. Proc Natl Acad Sci USA. 2000;97:12595–12600.
28. Melgar-Lesmes P, Edelman ER. Monocyte-endothelial cell interactions in the regulation of vascular sprouting and liver regeneration in mouse. J Hepatol. 2015;63:917–25.
29. Wen Y, Feng D, Wu H, Liu W, Li H, Wang F, et al. Defective initiation of liver regeneration in osteopontin-deficient mice after partial hepatectomy due to insufficient activation of IL-6/Stat3 pathway. Int J Biol Sci. 2015;11:1236–47.
30. Shan Z, Ju C. Hepatic macrophages in liver injury. Front Immunol 2020;11:322.
31. Abshagen K, Eipel C, Kalff JC, Menger MD, Vollmar B. Loss of NF-κB activation in Kupffer cell-depleted mice impairs liver regeneration after partial hepatectomy. Am J Physiol Liver Physiol. 2007;292:1570–7.
32. Meijer C, Wiezer MJ, Diehl AM, Yang S-Q, Schouten HJ, Meijer S, et al. Kupffer cell depletion by CI2MDP-liposomes alters hepatic cytokine expression and delays liver regeneration after partial hepatectomy. Liver. 2000;20:66–77.
33. Böhm F, Köhler UA, Speicher T, Werner S. Regulation of liver regeneration by growth factors and cytokines. EMBO Mol Med. 2010;2:294–305.
34. Blindenbacher A, Wang X, Langer I, Savino R, Terracciano L, Heim MH. Interleukin 6 is important for survival after partial hepatectomy in mice. Hepatology. 2003;38:674–82.
35. Schmidt-Arras D, Rose-John S. IL-6 pathway in the liver: from physiopathology to therapy. J Hepatol. 2016;64:1403–15.
36. He Y, Hwang S, Ahmed YA, Feng D, Li N, Ribeiro M, et al. Immunopathobiology and therapeutic targets related to cytokines in liver diseases. Cell Mol Immunol. 2021;18:18–37.
37. Garbers C, Aparicio-Siegmund S, Rose-John S. The IL-6/gp130/STAT3 signaling axis: recent advances towards specific inhibition. Curr Opin Immunol. 2015;34:75–82.
38. Fazel Modares N, Polz R, Haghighi F, Lamertz L, Behnke K, Zhuang Y, et al. IL-6 trans-signaling controls liver regeneration after partial hepatectomy. Hepatology. 2019;70:2075–91.
39. Hou X, Yin S, Ren R, Liu S, Yong L, Liu Y et al. Myeloid cell-specific IL-6 signaling promotes miR-223-enriched exosome production to attenuate NAFLD-associated fibrosis. Hepatology. 2020; https://doi.org/10.1002/hep.31658.
40. Quintana A, Erta M, Ferrer B, Comes G, Giralt M, Hidalgo J. Astrocyte-specific deficiency of interleukin-6 and its receptor reveal specific roles in survival, body weight and behavior. Brain Behav Immunol. 2013;27:162–73.
41. He Y, Feng D, Hwang S, Mackowiak B, Wang X, Xiang X et al. Interleukin-20 exacerbates acute hepatitis and bacterial infection by downregulating Inhibitor of kappa B zeta; target genes in hepatocytes. J Hepatol. 2021. https://doi.org/10.1016/j.jhep.2021.02.004.
42. Schug TT, Xu Q, Gao H, Peres-da-Silva A, Draper DW, Fessler MB, et al. Myeloid deletion of SIRT1 induces inflammatory signaling in response to environmental stress. Mol Cell Biol. 2010;30:4712–21.
43. Sun Z, Klein AS, Radaeva S, Hong F, El-Assal O, Pan H, et al. In vitro interleukin-6 treatment prevents mortality associated with fatty liver transplants in rats. Gastroenterology. 2003;125:202–15.
44. Aparicio-Vergara M, Tencerova M, Morgantini C, Barreby E, Aouadi M. Isolation of Kupffer cells and hepatocytes from a single mouse liver BT—alpha-1 antitrypsin

deficiency: methods and protocols. In: Borel F, Mueller C (eds). New York, NY: Springer, 2017, pp 161–71.
45. Jenkins SJ, Ruckerl D, Cook PC, Jones LH, Finkelman FD, van Rooijen N, et al. Local macrophage proliferation, rather than recruitment from the blood, is a signature of TH_2 inflammation. Science. 2011;332:1284–8.
46. Wynn AA, Miyakawa K, Miyata E, Dranoff G, Takeya M, Takahashi K. Role of granulocyte/macrophage colony-stimulating factor in zymocel-induced hepatic granuloma formation. Am J Pathol. 2001;158:131–45.
47. Kim AR, Park JI, Oh HT, Kim KM, Hwang J-H, Jeong MG, et al. TAZ stimulates liver regeneration through interleukin-6–induced hepatocyte proliferation and inhibition of cell death after liver injury. FASEB J. 2019;33:5914–23.
48. Feng D, Dai S, Liu F, Ohtake Y, Zhou Z, Wang H, et al. Cre-inducible human CD59 mediates rapid cell ablation after intermedilysin administration. J Clin Investig. 2016;126:2321–33.
49. Scott CL, Zheng F, De Baetselier P, Martens L, Saeys Y, De Prijck S, et al. Bone marrow-derived monocytes give rise to self-renewing and fully differentiated Kupffer cells. Nat Commun. 2016;7:10321.
50. Vassiliou I, Lolis E, Nastos C, Tympa A, Theodosopoulos T, Dafnios N, et al. The combined effect of erythropoietin and granulocyte macrophage colony stimulating factor on liver regeneration after major hepatectomy in rats. World J Surg Oncol. 2010;8:57.
51. Liu H-X, Keane R, Sheng L, Wan, JY Y-. Implications of microbiota and bile acid in liver injury and regeneration. J Hepatol. 2015;63:1502–10.
52. Norris CA, He M, Kang L-I, Ding MQ, Radder JE, Haynes MM, et al. Synthesis of IL-6 by hepatocytes is a normal response to common hepatic stimuli. PLoS ONE. 2014;9:e96053.
53. Imperatore F, Maurizio J, Vargas Aguilar S, Busch CJ, Favret J, Kowenz-Leutz E, et al. SIRT1 regulates macrophage self-renewal. EMBO J. 2017;36:2353–72.
54. Jin J, Iakova P, Jiang Y, Medrano EE, Timchenko NA. The reduction of SIRT1 in livers of old mice leads to impaired body homeostasis and to inhibition of liver proliferation. Hepatology. 2011;54:989–98.
55. Hunter CA, Jones SA. IL-6 as a keystone cytokine in health and disease. Nat Immunol. 2015;16:448–57.

ACKNOWLEDGEMENTS

Yeni Ait Ahmed was a participant in the NIH Graduate Partnerships Program and a graduate student at the Université Paris-Est-Créteil, France, and is affiliated with the Université Paris-Est-Créteil (UPEC) and the NIH Graduate Partnerships Program. This work was supported by the intramural program of the NIAAA (Bin Gao), the NIH grant R01DK121330, R01DK 122708, R01DK122796 (Cynthia Ju), the Institut Universitaire de France (Fouad Lafdil), and the Ministerio de Economía y Competitividad and European Regional Development Fund RTI2018-101105-B-100 (Juan Hidalgo).

AUTHOR CONTRIBUTIONS

Y.A.A. designed and performed the surgical procedures and experimental work and wrote the paper. Y.F., R.M.R., Y.H., Y.G., A.G., R.R., and D.F. helped with the PHx surgery, cell isolation, protocol optimization, and other experiments. J.H. and C.J. helped analyze the data and edited the paper. F.L. and B.G. designed and supervised the study and wrote the manuscript.

COMPETING INTERESTS

The authors declare no competing interests.

ADDITIONAL INFORMATION

Correspondence and requests for materials should be addressed to F.L. or B.G.